V_e = minimum entrainment velocity (determined at the plunging point), cm./sec.
V_s = surface velocity of jet, cm./sec.
Z = jet length, cm.

Greek Letters

α = entrainment velocity ratio
γ = surface tension of liquid, dyne/cm.
μ = liquid viscosity, centipoise
ρ = liquid density, g./cc.

LITERATURE CITED

1. Birkhoff, G., and E. H. Zarantonello, "Jets, Wakes and Cavities," Academic Press, New York (1957).
2. Flack, J. E., J. I. Kveisengen, and J. H. Nath, *Science*, **134**, 392 (1961).
3. Hickox, G. H., *Civil Eng.*, **15**, 562 (1945).
4. Lane, E. W., *ibid.*, **9**, 88 (1939).
5. Straub, L. G., and A. G. Anderson, *Proc. Am. Soc. Civil Engs., Hydraulic Div.*, Paper 1890 (1958).
6. Straub, L. G., and O. P. Lamp, *Trans. Am. Soc. Civil Engs.*, **121**, 30 (1956).
7. Shirley, R. W., M.S. thesis, Univ. Iowa, Ames (1950).
8. Ohyama, Y., Y. Takashima, and H. Idemura, *Rept. Sci. Res. Inst. (Japan)*, **29**, 344 (1954).
9. Braun, I., and M. Reiner, *Quart. J. Mech. Appl. Math.*, **5**, 42 (1952).
10. Middleman, Stanley, D. Eng. dissertation, John Hopkins Univ., Baltimore (1961).
11. Philippoff, W., *Trans. Soc. Rheol.*, **1**, 95 (1957).
12. Lin, Tong Joe, Ph.D. dissertation, Wayne State Univ., Detroit (1963); Univ. Microfilms, No. 64-9539, Ann Arbor, Mich.
13. Hansen, R. S., M. E. Purchase, T. C. Wallace, and R. W. Woody, *J. Phys. Chem.*, **62**, 210 (1958).
14. Christiansen, R. M., and A. N. Hixson, *Ind. Eng. Chem.*, **49**, 1017 (1957).

Manuscript received April 14, 1965; revision received December 13, 1965; paper accepted December 15, 1965. Paper presented at A.I.Ch.E. Philadelphia meeting

Bubble Growth by Dissolution: Influence of Contact Angle

W. M. BUEHL and J. W. WESTWATER

University of Illinois, Urbana, Illinois

The rate of growth of bubbles forming on a wall from a liquid initially uniformly supersaturated with a dissolved gas was investigated. Attention was directed to the effect of the contact angle.

Theoretical predictions for the growth rate of a spherical bubble tangent to a wall were carried out with a digital computer. The predictions included the diffusion equation and the continuity equation. The energy equation was neglected; viscosity and surface tension were assumed nil. The results are compared with existing predictions for a 90-deg. contact angle. For extremely slow growth, the theoretical growth coefficient is about 30% smaller for a bubble with zero contact angle compared to one with a 90-deg. contact angle. For fast growth the difference is much less.

Experimental growth rates were determined photographically for bubbles of carbon dioxide coming out of solution from water at an artifical nucleation site. Different contact angles from 15 to 89 deg. were obtained by coating the wall with various nonwetting agents. Every bubble showed changes in its contact angle during growth. No effect of contact angle on the growth rate could be detected.

In recent years there has been much interest in the growth of bubbles in liquids, particularly in connection with the problems of heat transfer during boiling. Theoretical predictions have been given by Bosnjakovic (*1*), Epstein and Plesset (*2*), Forster and Zuber (*3*), Plesset and Zwick (*4*), Griffith (*5*), Bankoff and Mikesell (*6, 7*), Birkhoff, Margulies, and Horning (*8*), Scriven (*9*), Bruijn (*10*), Forster (*11*), Skinner and Bankoff (*12, 13*), Yang and Clark (*14*), Han and Griffith (*15*), and others. Experimental measurements have been published by Fritz and Ende (*16*), Dergarabedian (*17*), Manley (*18*), Doremus (*19*), Strenge, Orell, and Westwater (*20*), Westwater and Westerheide (*21*), Van Wijk and Van Stralen (*22*), Houghton, Ritchie, and Thomson (*23*), Benjamin and Westwater (*24*), Patten (*25*), Glas and Westwater (*26*), and others. In many respects the actual conditions existing in a liquid (particularly a boiling liquid) are not the same as those assumed by the theoretical workers. A more lengthy discussion of this is given elsewhere (*27, 28*). The exact conditions existing in a practical system are so complex that a complete analytical solution probably never will be obtained.

To bridge the gap between theory and experiment, it is necessary to determine which of the differences between real and ideal conditions are important and which are trivial. One of the common assumptions used in theoretical works is that growing or collapsing bubbles are spheres in an infinite body of liquid. An equivalent assumption used frequently (*5, 11*) is that the bubbles are hemispheres in contact with a frictionless plane in a semi-

W. M. Buehl is with Corning Glass Works, Corning, New York.

infinite liquid. Of course in real systems bubbles on a wall are very common, but a contact angle of 90 deg. is not common.

In general, the question of contact angle is ignored or brushed aside lightly in the literature. Even predictions such as those by Griffith (*5*) and Forster (*11*) for growth in liquid with an asymmetric temperature distribution start with a hemispherical bubble on the wall. The reasoning expressed by Griffith is that, "a hemispherical shape is simple and easy to handle analytically." Griffith evidently felt either that growth for any other contact angle was too difficult to calculate or that it was not sufficiently different from the hemispherical case to justify the additional calculational effort.

One estimate of the effect of contact angle is found in the work of Manley (*18*). He refers to it as the wall effect and uses at factor of $(\ln 2)^{-1}$ to correct for it. This factor is found from the electrical capacitance of a sphere tangent to a conducting plane, and will be shown in this paper to apply only for very restrictive conditions.

The object of this study was to give attention to the contact angle, and to show the direction and magnitude of the possible error in predictions based on a 90-deg. contact angle if the contact angle is not 90 deg. In particular the asymptotic growth rate was calculated for the extreme case of a spherical bubble tangent to a wall (contact angle of zero).

In addition, experimental measurements were carried out, starting with a supersaturated solution of carbon dioxide in water. Release of the ambient pressure resulted in the growth of a bubble at an artificial nucleation site on a wall. Different contact angles, 15 to 89 deg., were obtained by using different surface treatments on the wall. For this system the bubble growth rate is controlled by mass diffusion. The analogy between heat conduction and mass diffusion may be used to extend the results to bubble growth in pure boiling liquids.

THEORY

Numerous papers have demonstrated that for a wide variety of systems the pressure inside a bubble growing in a superheated or supersaturated liquid is practically the same as the pressure in the ambient liquid. Thus for an isothermal, supersaturated liquid solution, the rate of bubble growth is controlled by the rate of mass diffusion to the bubble wall. Some other assumptions will be employed: the liquid has a constant density, no chemical reactions occur, and the heat of solution is nil. The concentration of the dissolved gas at any point in the liquid is given by a mass balance, Equation (1).

$$\frac{\partial C}{\partial t} + V_x\frac{\partial C}{\partial x} + V_y\frac{\partial C}{\partial y} + V_z\frac{\partial C}{\partial z} = D\left(\frac{\partial^2 C}{\partial x^2} + \frac{\partial^2 C}{\partial y^2} + \frac{\partial^2 C}{\partial z^2}\right) \quad (1)$$

No assumption of spherical symmetry is used here. The initial and boundary conditions are chosen to be

$$C = C_\infty, \quad \text{everywhere at time zero} \quad (2)$$

$$C = C_\infty, \quad \text{as } x, y, \text{ or } z \to \infty, \text{ at all times} \quad (3)$$

$$C = C_s, \quad \text{at the bubble wall at all times} \quad (4)$$

The growth of the bubble may be expressed by a mass balance, Equation (5).

$$\rho_G\frac{dv}{dt} = \frac{D}{\left(1 - \frac{C_s}{\rho_L}\right)}\oint\frac{\partial C}{\partial n}\,dA \quad (5)$$

One cannot solve these equations without a knowledge of the flow pattern in the liquid. All prior writers have assumed true radial flow, because it is the easiest case. If this assumption is rejected, one can continue as follows. We shall restrict ourselves to the case of no forced convection. The velocities in Equation (1) must be determined by separate relations. For a nonviscous fluid a flow potential ψ may be determined such that

$$V_x = -(\partial\psi/\partial x) \quad (6a)$$

$$V_y = -(\partial\psi/\partial y) \quad (6b)$$

$$V_z = -(\partial\psi/\partial z) \quad (6c)$$

The potential must satisfy the Laplace expression, Equation (7), and the boundary condition, Equation (9), yet to be derived.

$$(\partial^2\psi/\partial x^2) + (\partial^2\psi/\partial y^2) + (\partial^2\psi/\partial z^2) = 0 \quad (7)$$

A new variable S, which describes the bubble surface, is a function of x, y, z, and t, and satisfies the relationship, Equation (8).

$$S(x, y, z, t) = 0 \quad (8)$$

The boundary condition at the bubble wall is satisfied by Equation (9).

$$\frac{\partial\psi}{\partial x}\frac{\partial S}{\partial x} + \frac{\partial\psi}{\partial y}\frac{\partial S}{\partial y} + \frac{\partial\psi}{\partial z}\frac{\partial S}{\partial z} = +\epsilon\frac{\partial S}{\partial t} \quad (9)$$

where

$$\epsilon = (\rho_L - \rho_G)/\rho_L \quad (10)$$

There is no way to eliminate time from these equations if the bubble changes shape arbitrarily. However, if the bubble has always the same shape as it changes in size, time may be eliminated by the following substitutions. Here h is some length parameter of the bubble and varies with time only.

$$x_o = x/h \quad (11a)$$

$$y_o = y/h \quad (11b)$$

$$z_o = z/h \quad (11c)$$

For a bubble which is a sphere or any segment of a sphere having a radius R, a satisfactory choice of h is

$$h = 2R \quad (12)$$

Consider a bubble, which is a segment of a sphere, on a wall such that the contact angle measured through the liquid is a constant α. The wall is considered to be insulating, that is, neither a source or a sink. The equation of the bubble surface, Equation (8), is found to be Equation (13).

$$S = x_o^2 + y_o^2 + (z_o - \tfrac{1}{2}\cos\alpha)^2 - \tfrac{1}{4} = 0 \quad (13)$$

The equation of the solid surface is

$$z_o = 0 \quad (14)$$

Let

$$\psi = 4\,R\,\dot{R}\,\psi_o \quad (15)$$

Then Equations (1), (5), (7), and (9) become Equations (16), (17), (20), and (21).

$$\frac{4R^2}{D}\frac{\partial C}{\partial t} - \frac{4R\dot{R}}{D}\left[\left(x_o + \frac{\partial\psi_o}{\partial x_o}\right)\frac{\partial C}{\partial x_o} + \left(y_o + \frac{\partial\psi_o}{\partial y_o}\right)\frac{\partial C}{\partial y_o} + \left(z_o + \frac{\partial\psi_o}{\partial z_o}\right)\frac{\partial C}{\partial z_o}\right] = \frac{\partial^2 C}{\partial x_o^2} + \frac{\partial^2 C}{\partial y_o^2} + \frac{\partial^2 C}{\partial z_o^2} \quad (16)$$

$$b\rho_G R\dot{R} = \frac{2D}{1 - \frac{C_o}{\rho_L}} \oint \frac{\partial C}{\partial n_o} dA_o \qquad (17)$$

where

$$b = \frac{3v}{R^3} = \pi (1 + \cos\alpha)^2 (2 - \cos\alpha) \qquad (18)$$

and

$$dA_o = \frac{dA}{4R^2} \qquad (19)$$

$$\frac{\partial^2\psi_o}{\partial x_o^2} + \frac{\partial^2\psi_o}{\partial y_o^2} + \frac{\partial^2\psi_o}{\partial x_o^2} = 0 \qquad (20)$$

$$\frac{\partial\psi_o}{\partial x_o} x_o + \frac{\partial\psi_o}{\partial y_o} y_o + \frac{\partial\psi_o}{\partial z_o} (z_o - \tfrac{1}{2}\cos\alpha) =$$
$$- \epsilon [x_o^2 + y_o^2 + z_o (z_o - \tfrac{1}{2}\cos\alpha)] \qquad (21)$$

Equations (16) to (21) may be used to solve the time-dependent case by numerical techniques. Moreover, time is readily eliminated if the growth is such that $R = 2\beta\sqrt{Dt}$ or

$$R\dot{R} = 2\beta^2 D = \text{constant} \qquad (22)$$

Equation (22) is the asymptotic growth case treated extensively in the prior literature which consider either isolated spheres far from any wall or hemispheres on a wall. In fact when the contact angle α is 90 deg. in the above equations, they may be combined with Equation (22) and solved exactly to yield the same results described by Scriven (9) or Birkhoff, Margulies, and Horning (8). When the contact angle is not 90 deg., no closed form solution exists, except for the limiting case when β approaches zero. For this case of $\beta \to 0$, a stationary bubble, the solution may be obtained by modifying the results given by MacDonald (29). MacDonald calculated capacitances in an electric field. His result is Equation (23) after the necessary modifications (30).

$$\frac{R\dot{R}}{D} = \frac{2\rho_L(C_\infty - C_s)\sin\alpha}{3b\rho_G(\rho_L - C_s)\sqrt{2}} \int_o^\infty \frac{1}{\sqrt{\cosh x - 1}} \cdot$$
$$\left\{ \frac{\frac{\pi}{2\alpha}\sinh\frac{\pi x}{2\alpha}}{\cosh\frac{\pi x}{2\alpha} - 1} - \frac{\frac{\pi}{2\alpha}\sinh\frac{\pi x}{2\alpha}}{\cosh\frac{\pi x}{2\alpha} + 1} - \frac{\sinh x}{\cosh x - 1} \right\} dx \qquad (23)$$

MacDonald shows that the integral may be expanded in a series. For $\alpha = 0$, the correction to β^2 for the spherically symmetric case is the factor ln 2 = 0.693. That is, a bubble tangent to a wall grows 69.3% as fast as a bubble of the same size remote from a wall. For a contact angle of 45 deg. the correction factor is 0.686. One must keep in mind that MacDonald's values are for small β, that is, the extreme case of negligible motion.

If β is not small, the flow field in the liquid must be considered. This case will now be considered. Equations (16) to (22) were solved by the use of finite-difference methods. The limiting case of a spherical bubble tangent to a wall will be presented.

The shape of the bubble makes cumbersome the use of rectangular coordinates; inverse cylindrical coordinates, defined below, are better.

$$x_o = \frac{s_1 \cos\theta}{s_1^2 + s_2^2} \qquad (24a)$$

$$y_o = \frac{s_1 \sin\theta}{s_1^2 + s_2^2} \qquad (24b)$$

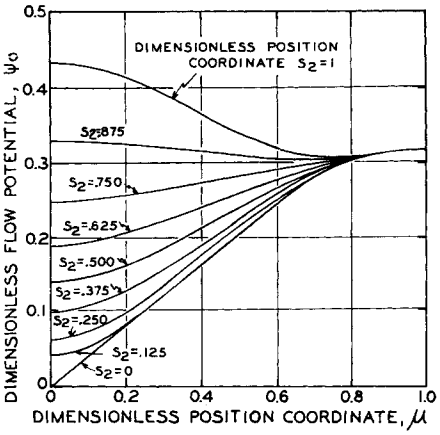

Fig. 1. Flow potential at all positions in the liquid surrounding a spherical bubble tangent to a wall. Dimensionless parameters are used.

$$z_o = \frac{s_2}{s_1^2 + s_2^2} \qquad (24c)$$

In these coordinates the equation of the bubble wall is $s_2 = 1$; the solid wall is given by $s_2 = 0$; the point of tangency is given by $s_1 = \infty$; and all points infinite distance from the bubble become the single point $s_1 = s_2 = 0$. We note that $s_1^2 + s_2^2 = S^2$. The effect of this transformation is to expand the region near the point of tangency and to contract the region far from the bubble.

Inasmuch as s_1 varies from 0 to ∞, a range not well suited to numerical computation, another substitution is convenient, Equation (25).

$$s_1 = \tan \mu\pi/2 \qquad (25)$$

A large digital computer was used to solve for the functionality of ψ_o on μ and s_2 for this case. The results are shown in Figure 1. In dimensionless form, with transformations as described above, this graph shows the flow potential at all positions in the liquid surrounding an expanding spherical bubble tangent to a wall. Detailed tables of the values to six significant figures are available (30).

After the flow potential field is known, it is reasonably straightforward to compute the values of the dimensionless growth coefficient β for various values of the dimensionless driving force Φ. The parameter Φ used here is the same as used by Scriven and is defined by Equation (26).

$$\Phi = \frac{\rho_L(C_\infty - C_s)}{\rho_G(\rho_L - C_s)} \qquad (26)$$

TABLE 1. COMPARISON OF THEORETICAL GROWTH RATES FOR CONTACT ANGLES OF 0 AND 90 DEG.
(for $\epsilon = 1.0$)

	$\alpha = 0°$		$\alpha = 90°$	
β	Φ	$\frac{2\beta^2}{\Phi}$	Φ	$\frac{2\beta^2}{\Phi}$
0.000	0.000	0.693	0.000	1.000
0.005	0.0000710	0.704	0.0000493	1.009
0.05	0.00643	0.778	0.00459	1.090
0.5	0.312	1.603	0.254	1.97
1.0	0.778	2.569	0.6977	2.96
1.5	1.26	3.55	1.175	3.83
2.0	1.76	4.55	1.668	4.80

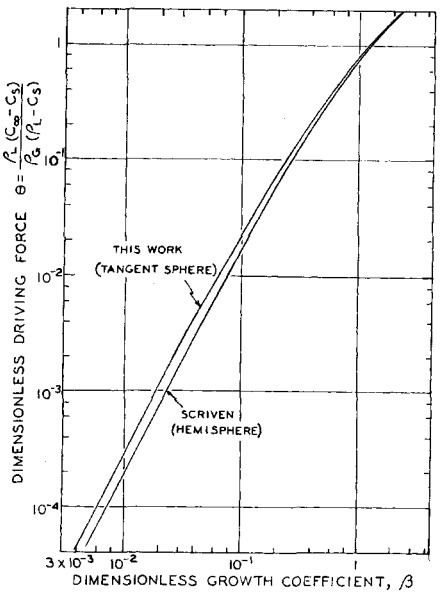

Fig. 2. Comparison of theoretical growth coefficient for a spherical bubble tangent to a plane and a hemispherical bubble on a plane, assuming the liquid density >> gas density. The hemisphere calculation is the same as for a remote sphere.

A selection of seven sets of β vs. Φ values is given in Table 1. The values for the tangent bubble on a frictionless wall are given under $\alpha = 0$. For comparison the case of spherical symmetry, that is, a hemisphere on a frictionless wall, is shown under $\alpha = 90$ deg. The values under $\alpha = 90$ were taken from Scriven's paper. The third and fifth columns in Table 1 compare the two cases quantitatively. The result is perhaps surprising; the effect of the contact angle on the bubble growth rate, at least for contact angles between 0 and 90 deg., amounts to a maximum difference of only 30.7%. This maximum effect occurs for infinitely slow growth, $\beta \to 0$. As the driving force is increased and β increases, the difference between the growth rates for the two contact angles becomes smaller. At $\beta = 2.0$, the two cases differ by only 5.2%. Figure 2 shows a comparison for the tangent sphere and the hemisphere.

The β vs. Φ values for the contact angle of zero can be interpolated with very good precision (to within 2% for β between zero and 2.0) by the empirical relationship (*30*), Equation (27).

$$\Phi = \frac{2\beta^2}{0.693 \left[\frac{(0.693)^2 + \frac{16}{9}\sqrt{\frac{3}{\pi}}\beta}{(0.693)^2 + 2\beta} \right] + 2\sqrt{\frac{3}{\pi}}\beta} \qquad (27)$$

Calculations on the digital computer were not carried out for cases with β greater than 2.0. The results in Table 1 indicate that the additional calculations would result in information of minor value only, that is, effects of less than 5%.

Concerning contact angles other than 0 or 90 deg., the growth constant may be computed by use of the differential equations given here. The rather small magnitude of the difference in growth rate for bubbles with 0- and 90-deg. contact angles is interpreted by the writers to mean that contact angle is a weak variable. For that reason the calculations were not extended to other angles.

The fact that contact angle is a weak variable when β is large means that the depletion of solute is restricted practically to a very thin shell around the growing bubble. For distances farther away, the concentration is nearly constant. Thus a film theory type of approach for rapidly growing bubbles seems rational. Such an approach has been used by some prior writers [Bankoff (*6, 7*) for example].

EXPERIMENTAL

In brief, a viewing cell was filled with water saturated with carbon dioxide at some pressure in the range 5 to 45 lb./sq.in. gauge; the pressure was then reduced to atmospheric and the solution thereby became supersaturated uniformly. A series of bubbles then appeared on a wall at a tiny artificial nucleation site. Motion picture photography was used to record the growth and contact angles of the bubbles.

The general features of the viewing cell are shown in Figure 3. The cell was machined from a copper block and was fitted with two parallel glass windows. The liquid chamber measured 2 in. × 1 in. × ⅝ in., but part of this volume was occupied by a 1.5-in. × 1-in- × ½-in. platform which contained a single artificial nucleation site in the center of the horizontal plane. The features of the design were such as to facilitate filling, emptying, and cleaning of the cell.

The nucleation site was a 0.004-in. diameter by 0.006-in. deep pit which connected to a 0.03-in. diameter by 0.03-in.-deep cavity below the surface. Drilling techniques, and also in some cases electric spark techniques, were used to obtain the pit. An artificial site, rather than natural ones, was used for the tests, because photography is simplified if the exact location of the target is known. In addition natural sites may vary enormously in size and shape, whereas artificial ones can be made approximately to one set of measurements. The interior of the test cell was polished with a 320-grit alumina powder to minimize the occurrence of natural sites. For some tests a few extraneous sites were evident; however, in other cases none existed.

The contact angle of the bubble on the wall was varied by use of various nonwetting coatings (paraffin, cupric oleate, oleic acid, stearic acid) on the copper. The resulting angle varied from 15 to 89 deg.

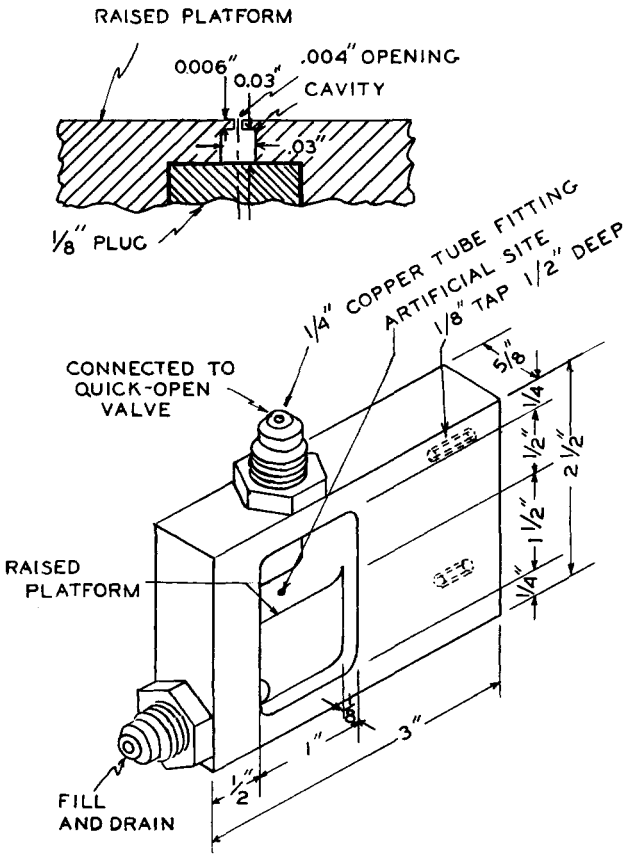

Fig. 3. Test cell with artificial nucleation site. The windows are removed in this view.

A mixing bomb was used for preparation of the distilled water–carbon dioxide solutions under pressure. A minimum of 8 hr. was allowed to establish saturation. Then the liquid was transferred to the test cell which had been kept at an absolute pressure of about 17 mm. Hg for at least 30 min. to remove all volatile material. Connections between the liquid-filled cell and the mixing bomb were kept open for 30 min. The valves between the cell and the bomb were then closed, photography was begun, a vent to the atmosphere was opened suddenly, and a timing mark was recorded on the movie film. The first bubble appeared at the nucleation site between 1/16 to 2 sec.

The bubbles were photographed at known framing rates between 14 and 17 frames/sec. with a Bolex Reflex 16-mm. motion picture camera. No lens was attached to the camera, but a 2-in. focal length, f/1.8 Wollensak lens was located between the camera and test cell so as to result in a size magnification of 1.5 on the photographic film. Illumination was provided by a 60-w. incandescent bulb located on the optical axis behind the back window. The lamp, test cell, lens, and camera were all aligned carefully on an optical bench. Kodak Plus-X negative film was used for all runs.

Further details concerning the apparatus and procedure and an enlargement of a typical film strip are available (*30*).

EXPERIMENTAL RESULTS

The experimental work was intended to test the predictions outlined in the Theory section concerning the effect of contact angle. The work was executed with care, and the numerical results are believed to be accurate. Nevertheless, for reasons discussed below, the results do not prove or disprove the theory. The data are discussed in this paper because they are the only known quantitative information concerning the growth of bubbles by dissolution resulting from release of pressure on a liquid containing a dissolved gas. The lack of data concerning this phenomenon is surprising, considering the number of times bubbles growing in carbonated beverages have been observed. A small selection of the present data is illustrated here. Detailed measurements of diameter vs. time and contact angle vs. time for ninety-nine bubbles are recorded (*30*).

The described method of growing bubbles had two particularly desirable features. The initial supersaturation was uniform throughout the liquid; second, its original value was known. This contrasts with the previously used method of generating bubbles by electrolysis (*21, 26*) or a possible scheme of generating bubbles by chemical reaction between dissolved constituents. For these latter cases the initial supersaturation is not uniform and is not known.

However, with the present tests four nonidealized features became evident as soon as the first tests were completed. Two of these may be minimized by modifications in the test equipment. The third and fourth ones are much more vexing, and no realistic solution to them has been proposed.

The first of these features is that the bubbles originated at traces of compressed gas contained in the artificial site and expanded in part because of dissolution, but also in part because of simple pressure difference. This meant that most bubbles grew too fast during their first period of growth. This is evident in Figure 4. Growth during the later periods sometimes was normal, that is, the radius increased according to the square root of time. The possibility of expansion of trapped gas in the active site had been anticipated, and the vacuum degassing of the test cell prior to liquid filling was intended to minimize this complication. A perfect (100%) degassing of a nucleation site is not desired, because a tiny speck of gas is the birthplace of the bubbles being studied. An additional means of reducing the volume of the trapped gas is to reduce the volume of the artificial cavity by several orders of magnitude. This would be exceedingly difficult to do, but it does seem possible. Presumably, the site would have to be made by some means which avoids the use of drilling or cutting tools.

The second interesting complication was that the bubbles were not segments of spheres. The bubbles were tear-shaped with axial symmetry. Their volumes were found by a laborious procedure of computation by using seven measurements and assuming a true solid of revolution. For graphing purposes a mean radius was defined as $(V/\pi)^{1/3}$. This gives 0.87 times the true radius for a sphere and 1.10 times the true radius for a hemisphere; therefore, it is a useful compromise. However, the deviation of the bubble shape from that of a spherical segment makes very difficult (or questionable) comparisons with the theoretical prediction. To solve this difficulty one must use much smaller bubbles. This requires the use of nucleation sites much smaller than the 0.004-in. diameter used herein.

The third complication is illustrated by Figure 4. This graph shows the growth data and contact angle data for run 3A which was carried out by decreasing the pressure from 40.2 lb./sq. in. gauge to atmospheric pressure. Seven bubbles formed in succession at the artificial nucleation site. The first grew rapidly. Its mean radius upon its first appearance was 0.588 mm., and it broke loose after achieving a mean radius of 1.29 mm. in a growth time of 1.89 sec. Next occurred a waiting time of 1.05 sec., and then bubble 2 appeared. Its growth time was 6.37 sec. Bubble 3 had a waiting time of 4.20 sec. and a growth time of 6.92 sec. Every successive bubble had a longer waiting time and a slower growth rate than its predecessor. For bubble 7, these numbers reached 7.7 and 26.9 sec. The latter growth time is larger than the growth time of bubble 1 by a factor of 14, although the breakoff diameters were comparable. The logical explanation is that a steady depletion of solute was occurring. However, for this run, the excess solute available in solution in the test cell at time zero was enough to account for about four thousand bubbles having a radius of 1.2 mm. Thus the solute depletion during the first seven bubbles was entirely localized. This means that the liquid pool was more or less stagnant and that the stirring action of the bubbles was negligible.

For boiling liquids the stirring action of the growing bubbles seems to be significant. Bubbles in boiling liquids grow about a thousand times faster than bubbles forming by dissolution. This is to be expected because diffusivity of heat is much greater than diffusivity of mass.

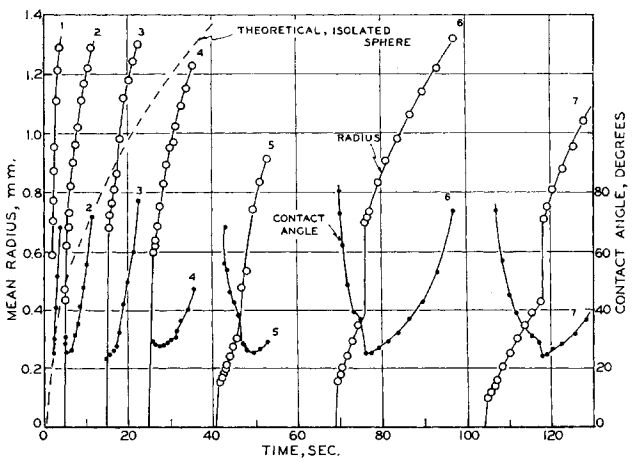

Fig. 4. Radius and contact angle for seven successive bubbles of carbon dioxide forming at artificial nucleation site. Pressure on the saturated aqueous solution of 42 lb./sq. in. gauge was changed to atmospheric at time zero.

The lack of mixing in the present runs poses a dilemma. It means that bubbles appearing after the first one are not suited for testing the present analysis, because the solute concentration in the nearby liquid is unknown. On the other hand, the first bubble grows in a well-defined concentration field. But the first bubble, as well as several successive ones, grows too fast as a result of the pressure impulse discussed earlier.

In Figure 4 the theoretical growth curve is shown. The diffusion coefficient used was 2.00×10^{-5} sq. cm./sec. from Scriven and Pigford (*31*), and solubilities were interpolated from the tables of Landolt-Börnstein (*32*). The theoretical line originates at time zero for the run. For any bubble in this graph, a comparison may be made by shifting the experimental bubble curve along the time axis to zero time. On this basis all the bubbles grow too fast at their start. The first few bubbles are too fast during their entire growth, but bubbles 5 and 6 in their late periods are near the theoretical prediction. Bubble 7 grows slower than predicted in its late period. Bubbles 6 and 7 were affected somewhat by coalescences with neighbors as can be detected from their growth curves. For the conditions of Figure 4 the theoretical growth coefficient β is 2.43. The experimental β varied from about 7.3 for bubble 1 to about 2.2 for bubble 7.

The fourth complication is that not one bubble maintained a constant contact angle during its growth. Figure 4 shows the contact angle changing by as much as 55 deg. during the life of bubble 6. The area of attachment of each bubble changes with time in a discontinuous manner as the bubble grows. For some bubbles the contact angle decreased as the bubbles grew, for some it increased, and for many it decreased and then increased; Figure 4 illustrates several of these cases. Electrolytic bubbles (*26*) also show changing contact angles during growth; usually the angle decreases as the bubble grows.

CONCLUSION

The conclusion from the theoretical work here is that the effect of contact angle on bubble growth rates during dissolution is very small, at least in the range of 0 to 90 deg. The experimental work indicates that factors other than contact angle are much more important, at least for contact angles in the range of 15 to 89 deg. These outcomes are fortunate, inasmuch as prior theoretical and experimental workers have assumed the effect of contact angle to be negligible.

ACKNOWLEDGMENT

Financial support was provided by the National Science Foundation. Graduate fellowships were furnished by the Monsanto Company and the Shell Oil Company.

NOTATION

A = gas-liquid interfacial area of a bubble, L^2
A_o = defined by Equation (19)
b = defined by Equation (18)
C = solute concentration in liquid phase, M/L^3
C_s = solute concentration in the liquid at the bubble wall, M/L^3
C_∞ = solute concentration far away in the liquid, M/L^3
D = mass diffusivity, L^2/t
h = selected length parameter, varies with time, L
n = distance normal to bubble wall, L
R = radius of bubble, L
S = transformation variable, Equation (13)
s_1,s_2 = transformation variables for inverse cylindrical coordinates, Equations (24*a*), (24*b*), (24*c*)
t = time, t
v = bubble volume, L^3
V_x,V_y,V_z = velocity along rectangular axes, L/t
x,y,z = rectangular coordinates, L
x_o,y_o,z_o = dimensionless rectangular coordinates

Greek Letters

α = contact angle, measured through the liquid
β = dimensionless growth coefficient, defined by $R = 2\beta\sqrt{Dt}$
ϵ = $1 - (\rho_G/\rho_L)$, dimensionless
θ = coordinate angle, origin is center of bubble
μ = transformation variable, defined by Equation (25)
ρ_G,ρ_L = density of gas, liquid, M/L^3
Φ = dimensionless concentration driving force, defined by Equation (26)
ψ = fluid flow potential, defined by Equation (6)
ψ_o = dimensionless flow potential defined by Equation (15)

LITERATURE CITED

1. Bosnjakovic, F., *Tech. Mech. Therm.*, **1**, 358 (1930).
2. Epstein, P. S., and M. S. Plesset, *J. Chem. Phys.*, **18**, 1505-1509 (1950).
3. Forster, H. K., and Novak Zuber, *J. Applied Phys.*, **25**, 474 (1954).
4. Plesset, M. S., and S. A. Zwick, *ibid.*, 493.
5. Griffith, P., *Trans. Am. Soc. Mech. Engrs.*, **80**, 721 (1958).
6. Bankoff, S. G., and R. D. Mikesell, *Am. Soc. Mech. Engrs., Paper 58-A-105* (1958).
7. ———, *Chem. Eng. Progr. Symposium Ser. No. 29*, **55**, 95 (1959).
8. Birkhoff, G., R. S. Margulies, and W. A. Horning, *Phys. Fluids*, **1**, 201 (1958).
9. Scriven, L. E., *Chem. Eng. Sci.*, **10**, 1-13 (1959).
10. Bruijn, P. I., *Physica*, **26**, 326 (1960).
11. Forster, K., *Phys. Fluids*, **4**, 448 (1961).
12. Skinner, L. A., and S. G. Bankoff, paper presented at A.I.Ch.E. Natl. Meeting, Boston (December, 1963).
13. ———, *Phys. Fluids*, **7**, No. 1, 1-6 (1964).
14. Yang, Wen-Jei, and J. A. Clark, *Trans. Am. Soc. Mech. Engrs.*, **86C**, 207 (1964).
15. Han, Chi-Yeh, and Peter Griffith, *Rept. 7673-19*, Dept. Mech. Eng., Massachusetts Inst. Technol. (1962).
16. Fritz, W., and W. Ende, *Phys. Z.*, **37**, 401 (1936).
17. Dergarabedian, P., *J. Appl. Mech.*, **20**, 537 (1953).
18. Manley, D. J. M. P., *Brit. J. Appl. Phys.*, **11**, 38 (1960).
19. Doremus, R. H., *J. Am. Cer. Soc.*, **43**, 655-661 (1960).
20. Strenge, P. H., Aluf Orell, and J. W. Westwater, *A.I.Ch.E. J.*, **7**, 578-583 (1961).
21. Westerheide, D. E., and J. W. Westwater, *ibid.*, 357-362.
22. Van Wijk, W. R., and S. J. D. Van Stralen, *Physica*, **28**, 150 (1962).
23. Houghton, G., P. D. Ritchie, and J. A. Thomson, *Chem. Eng. Sci.*, **17**, 221-227 (1962).
24. Benjamin, J. E., and J. W. Westwater, *Proc. 1961-1962 Intern. Heat Transfer Conf.*, 212-218, Am. Soc. Mech. Engrs., New York (1963).
25. Patten, T. D., paper No. 9 presented at Thermodynamics and Fluid Mechanics Convention, Inst. Mech. Engrs., London (1964).
26. Glas, J. P., and J. W. Westwater, *Intern. J. Heat Mass Transfer*, **7**, 1427 (1964).
27. Westwater, J. W., "Research in Heat Transfer," J. A. Clark, ed., pp. 61-73, Pergamon Press, New York (1963).
28. ———, "Cavitation in Real Liquids," Robert Davies, ed., pp. 34-54, Elsevier, Amsterdam (1964).
29. MacDonald, H. M., *Proc. London Math. Soc.*, **26**, 156 (1895).
30. Buehl, W. M., Ph.D. thesis, Univ. Illinois, Urbana (1963).
31. Scriven, L. E., and R. L. Pigford, *A.I.Ch.E. J.*, **4**, 439 (1958).
32. Landolt-Börnstein, "Phys.-Chem. Tabellen," 5 ed., Springer, Berlin (1931).

Manuscript received April 26, 1965; revision received January 14, 1966; paper accepted January 17, 1966.